ORIGINAL ARTICLE

Eco-dyeing and functional finishing of wool fabric based on Portulaca oleracea L. as colorant and Musa basjoo as natural mordant

Wei Zhang [a,*], **Xin Wang** [a], **Jiali Weng** [a], **Xinwei Liu** [b], **Shaoxuan Qin** [c], **Xiaoyan Li** [a], **Jixian Gong** [b]

[a] *College of Textile and Garments, Hebei University of Science and Technology, China*
[b] *School of Textile Science and Engineering, Tiangong University, China*
[c] *Shanghai Academy of Fine Arts, Shanghai University, China*

Abstract Biomass energy is the most acknowledged renewable resource due to its universality, richness, and renewability. This study utilized a Portulaca oleracea L. plant as a natural colorant for wool fabric dyeing with a high color yield at optimum extraction and dyeing conditions. To evaluate the dyeing mechanism and feasibility of the extracted dyes, we analyzed and characterized the molecular structure and nano-level particle size. The dyeing kinetics and the morphology of dyed fabrics were integratedly explored; the adsorption process of wool fabric on natural colorant molecules was increasingly in line with the pseudo-second-order kinetic adsorption model. Further, the dyeing effects of wool fabrics were compared to that of Musa basjoo mordant and synthetic dyes to confirm the superior color depth (K/S value 23.53), biological function as anti-ultraviolet (UPF value 253.47), and anti-bacterial activity (antibacterial rate of *Staphylococcus aureus*/*Escherichia coli* was 71.3%/37%). Our findings provide a feasible scheme for providing deep color and biological activity to wool fabrics. This has broad application prospects in the field of eco-friendly textile materials.

* Corresponding author at: College of Textile and Garments, Hebei University of Science and Technology, NO.26 Yuxiang Street, Yuhua District, Shijiazhuang 050018, China.
E-mail address: weizhang@hebust.edu.cn (W. Zhang).
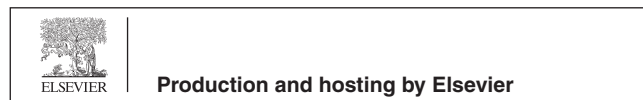
1. Introduction

With the advancement of global living standards, consumers focus on style and color, environmental protection as well as health when acquiring wearable textiles (Shahid et al., 2013; Zhou and Tang, 2017). Natural dyes are extensively used in antibacterial finishing, UV protection, and other fields due to their non-toxic, environmental protection, and multi-functional properties including antibacterial, anti-ultraviolet, and insect repellent (Safapour et al., 2018, Mr et al., 2021; Tang et al., 2016). Due to its unique appearance style, i.e. soft

feel, bright color, plump plush and excellent warmth retention, wool fabric is the first choice for high-end suits and coats (Luo et al., 2018). Considering ecological security and protection, scientists in the textile field are constantly searching for novel plants as natural dyes to produce high value-added wool fabrics exhibiting anti-insect and anti-bacterial properties (Baliarsingh et al., 2012, Ibrahim et al., 2015).

Portulaca oleracea L. is a dual-purpose herb for medicine and food. It is rich in fatty acids, vitamins and other nutrients. It is widely used in biology, medicine and other fields. It has anti-aging, analgesic, anti-inflammatory and neuroprotective effects. In addition, Portulaca oleracea L. has strong inhibitory effects on Escherichia coli, Staphylococcus aureus and other bacteria, and has strong biological activities in antibacterial, anti-inflammatory, anti allergic and anti-oxidation (Aludatt et al., 2020). Boris Nemzer et al. extracted 184 compounds in Portulaca oleracea L., including phenolic acids, organic acids, flavonoids, and alkaloids, among them, α-linolenic acid, quercetin, p-coumaric acid, catechin, kaempferol, and tannic acid were the primary active ingredients of the observed medicinal properties of leaves (Fig. 1) Petropoulos et al., 2016; Lm et al., 2019; Nemzer et al., 2020). These components have strong biological properties such as anti-bacterial, anti-inflammatory, anti-allergy, and prevention of diabetic complications (Hosseinzadeh et al., 2021; Oh et al., 2021; Ye et al., 2021). At present, researches on Portulaca oleracea L. are focused on the physical and chemical properties and antioxidant activity of its seed, leaf and stem, as well as its application in food and biomedicine (Desta et al., 2020; Seif et al., 2019; Wang et al., 2020).

The traditional health care fabrics are made by dyeing with acid and reactive dyes and finishing with antibacterial and anti-inflammatory additives (Eid and Ibrahim, 2020; Kenawy et al., 2007). The process is complicated, complex, high cost, and has a great stimulating effect on the skin. Natural dyes are organic macromolecules, and their intermolecular binding ability (intermolecular force or hydrogen bond) with nature fibers is general. In order to improve the color fastness, metal mordants are widely used, especially chromium mordants. However, the chromium-containing mordants will cause chromium pollution to the environment, which is a very serious problem. It is necessary to searching for an ecotype material as an alternative to a metal medium. Natural mordants are usually the substances containing tannins and ionic structuresin plants (Ylj et al., 2021). Aline Pereira et al found that Musa basjoo contains anthraquinone, flavonoids, coumarins, phenols, cyanide, amine, coumarin and other chemicals, which can simultaneously interact with certain dyes and fabric macromolecules (Pereira and Maraschin, 2015). The leaves, bark and fruit rinds of Musa basjoo have been used for dyeing of textiles as mordanting agent. The cell sap of Musa basjoo contain a considerable amount of tannin, which could stain the textile in almost dark black color (Mathur and Gupta, 2003). Tannin compounds are water-soluble polyphenols, which is composed of phenolic groups and aromatic rings. These active agents have the advantages of environmentally-friendly and safe to use, as well as antioxidant and antimicrobial capacity (Cano et al., 2021). Therefore, the tannin in Musa basjoo leaves can be used as a mordant to realize ecological dyeing and endow wool fabrics with functionality at the same time.

Herein, the wool fabric was considered a research object, and the colorant of purslane was extracted using the water-boiling method. The optimal colorant extraction and the dyeing processes were determined through the Statistical Product and Service Solutions (SPSS) design. The molecular structure and particle size of the extracted dyes were analyzed and characterized to investigate the dyeing mechanism and feasibility. Additionally, we comprehensively characterized the dyeing effect, functional and biological properties of the dyed wool fabric based on the color characteristic, rubbing fastness, antibacterial, anti-oxidation, and anti-ultraviolet properties. We are confident that purslane can become an eco-friendly, biologically active finishing agent and effective colorants for wool fabrics.

2. Experimental

2.1. Materials and chemicals

The Portulaca oleracea L. plant grows in Anhui Province, China. Wool fabric was purchased from Jiangsu Lugang Wool Textile Printing and Dyeing Co., Ltd. with the following specifications: Warp and weft: 17.2×17.2 tex; warp density: 216 threads per 10 cm; weft density: 184 threads per 10 cm, and weight: 224 g/m^2. Fresh Musa basjoo leaves were produced in Deqing County, Guangdong Province.

Staphylococcus aureus CMCC (b) 26,003 and E. coli CMCC (B) 44,102 were provided by the National Center for Medical
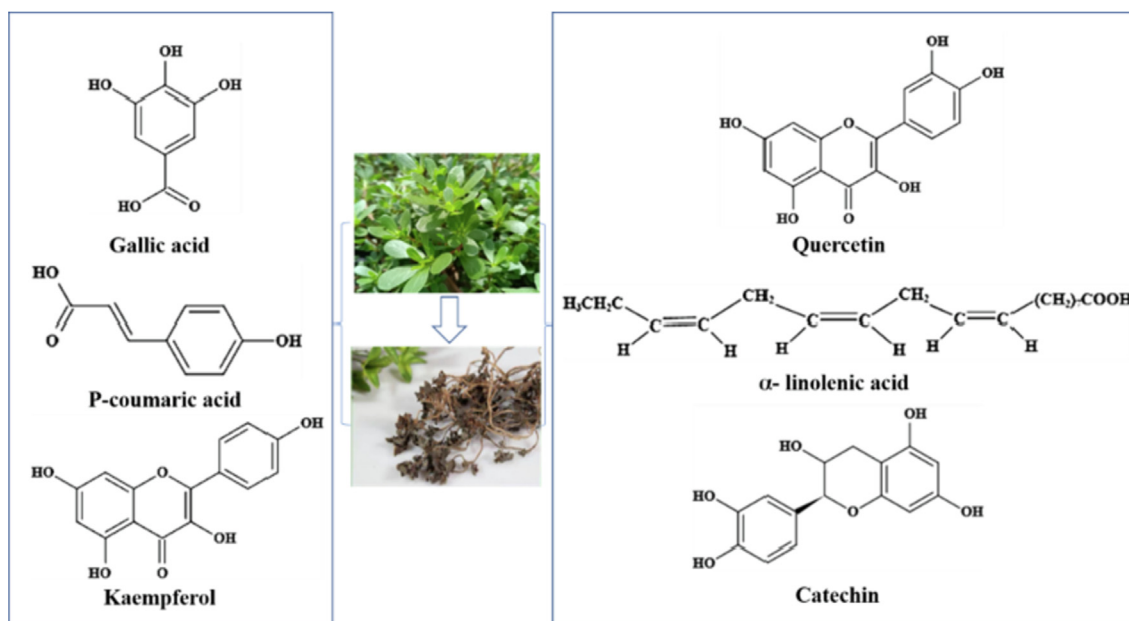

Fig. 1   The main active ingredients in Portulaca oleracea L.

Culture Collections. The nutritional broth was purchased from Beijing Aoboxing Biotechnology Co. Ltd.

Synthetic dyes including cerulein golden CE-01, cerulein blue 3G, cerulein red 6G were provided by Tianjin Sanhuan Chemical Co., Ltd. 1,1-diphenyl-2-trinitrophenylhydrazine was purchased from Fuzhou Feijing Biotechnology Co., Ltd. Acetic acid (HAC) was used for pH adjustment. The analytical reagents including anhydrous sodium carbonate (Na_2CO_3), anhydrous ethanol (C_2H_5OH), ammonium sulfate ((NH_4)$_2$-SO_4), were obtained from Tianjin Yongda Chemical Reagent Co. Ltd., China.

2.2. Methodology

2.2.1. Extraction of Portulaca oleracea L. colorant

The natural colorant of Portulaca oleracea L. was extracted by water bath method, and the absorbance of the extracted dye was determined by UV–vis spectrophotometry in the wavelength range of 320–400 nm. We analyzed the effects of different extraction conditions on the extraction efficacy of Portulaca oleracea L., including temperature (60–100 °C), time (0.5 h–2.5 h), solid–liquid bath ratio 2.5–5 g/100 mL H_2O (25.0–50.0 g/L). With temperature, time, and bath ratio as influencing factors, SPSS design was used to explore the optimal extraction process of Nd. The obtained filtrate was evaporated at room temperature, and the extracted dye powder was stored at low temperature (4 °C) for further analysis of components and functional groups.

2.2.2. Dyeing WF with natural dyes

The single factor optimization was used to explore the dyeing parameters, including pH (2–6), temperature (60–100 °C), dye concentration (1:20–1:40), and dyeing time (30–90 min). The dyed wool fabric (WF) was named naturally dyed fabric (NF).

2.2.3. Adsorption dynamics

Wool fabric was dyed at 80 °C, 90 °C, and 100 °C, respectively for a certain period to explore the adsorption kinetics of Nd on WF (Rather et al., 2017; Schaumlffel et al., 2021).

The isotherm method was used to dye the wool fabric at 80 °C, 90 °C, and 100 °C for a certain period to detect the adsorption kinetics of the Nd on the wool fabric.

$$q_t = (C_0 - C_t)\frac{V}{W} \tag{1}$$

where Co is the initial Nd concentration (g/L), C_t is the Nd concentration (g/L) at time t, V is the Nd volume (L), and W is the weight of WF (Kg).

2.2.4. Mordant dyeing WF with Musa basjoo

Naturally dyed fabric samples were dyed with 3.5% Musa basjoo leaf natural mordant to obtain MF (Mordant dyed fabric) (Kang et al., 2019; Zhang et al., 2021). The dye discharge under the optimum dyeing conditions (pH, temperature, dye concentration, and dyeing time) was measured at the maximum absorption wavelength of the Nd solution. The exhaustion rate was calculated as follows (Mathur and Gupta, 2003):

$$Exhaustion rate(\%) = \frac{A_0 - A_1}{A_0} \times 100 \tag{2}$$

where A_0 and A_1 are the absorbances of the dye solution before and after dyeing, respectively.

2.2.5. Dyeing WF with synthetic dyes

The synthetic dyes are used to compare the dyeing strength and functional properties of fabrics with that of natural dyed fabrics to evaluate the advantages of eco-dyeing and functional finishing of Portulaca oleracea L. as natural dyes. In order to obtain the same color as NF and MF, synthetic dye (Sd) baths were prepared with 1.28% CE-01, 0.17% CE-blue 3G and 0.23% CE-6G, and WF was dyed based on the process shown in Fig. 2 to obtain synthetic dyed fabric (SF) samples. The assistant comprised two drops of ring coeven B, 2% ammonium sulfate, and 0.15 mL HAc.

2.3. Characterization

The visible spectrophotometer (V-5600, Shanghai Yuanshi Instrument Co., Ltd., China) was used for spectral scanning of Nd at a wavelength range of 320–400 nm. The chemical groups of extracted Nd were analyzed using the Infrared-Raman spectrometer (Nicolet 6700/FT-Raman modules, Thermo Fisher, USA); the infrared spectra of WF, NF, and MF were collected at the wavelength range of 600 cm^{-1}–4000 cm^{-1} by Thermo Nicolet Is10 Fourier transform infrared spectrometer. Transmission electron microscopy (FEI Talos F200s, USA) was used to observe the size and shape of Nd particles. The surface morphology of WF, NF, and MF and the distributed elements on the surface was recorded using an electron microscope analyzer (Bruker nano Berlin, Germany) equipped with XFlash 6T|30 detectors. The K/S and L^*, a^*, b^*, c^*, h^o values of wool fabrics at 340 nm wavelength under different dyeing processes were measured by computer color matching instrument (Color i 5D, American Datacolor). The wash fastness of dyed woolen yarn samples was measured in Digi wash SSTM (Launder-o-meter) as per the ISO 105-C06:1994 (2010) specifications. The wet and dry rubbing fastness were tested based on ISO 105-X16-2002. The colorfastness to sunlight was rated according to ISO 105-B02-2013. The ultraviolet protection factor (UPF) and ultraviolet transmittance (UVA and UVB) were measured on the textile ultraviolet protection performance tester (YG909-III, Wenzhou Fangyuan Instrument Co., Ltd.).

The antibacterial properties of WF, NF, MF, and SF samples were tested using S. aureus and E. coli as test strains following the GB/T 20944.3–2008 "textile antibacterial performance evaluation method". The bacteriostatic rate was calculated based on Formula (3):

$$Y = \frac{W_t - Q_t}{W_t} \times 100\% \tag{3}$$

Y represents the antibacterial rate, W_t and Q_t are the average colonies from three control nutritional plates (CFU/mL) and dyed wool (CFU/mL), respectively.

In vitro, antioxidant activity was evaluated by the DPPH radical scavenging assay based on Ivan Best with modifications. Briefly, 50 μL of Nd, mordant dye, synthetic dyes extract was mixed with 950 μL DPPH (65 μmol/L in ethanol), then shaken for 10 min to completely dissolve DPPH. The wool fabric was placed in the mixture and reacted in dark for
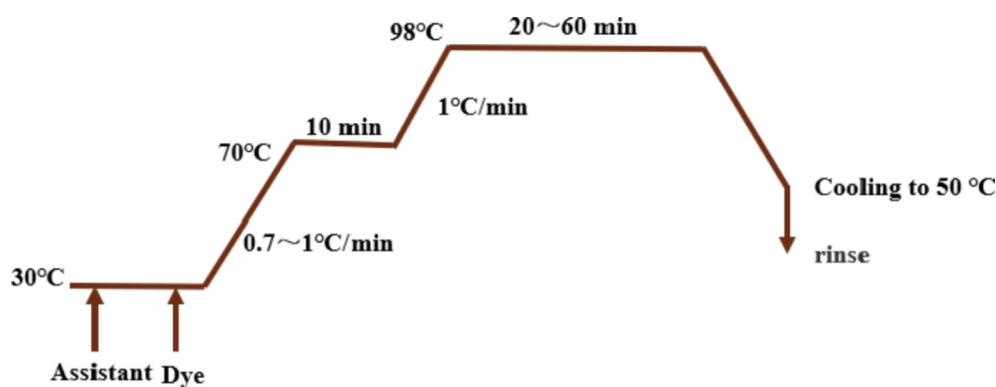
Fig. 2 Dyeing process flow chart of WF with synthetic dyes.

30 min. Then, a small amount of DPPH ethanol solution was transferred into a 10 mm colorimetric dish (Ren et al., 2021). The absorbance was measured by a UV spectrophotometer at 517 nm. The free radical scavenging efficacy of DPPH was calculated using Formula (4) (Iba et al., 2020):

$$\text{Free radical scavenging efficiency} = \frac{1 - A}{A_0} \times 100\% \qquad (4)$$

where A_0 is the absorbance of blank DPPH, and A is the absorbance of the sample.

3. Results and discussion

3.1. Chemical composition of Nd powder

The major active components in Portulaca oleracea L. include α-linolenic acid, quercetin, p-coumaric acid, catechin, and tannic acid. Generally, quercetin (flavonols) is largely gray-yellow. In the quercetin molecules, the introduction of ─OH and ─OCH$_3$ and other auxochromes at the 7-site and 4-site promotes electron transfer and rearrangement, resulting in the darker color of the compound as brownish-yellow (Fig. 3) (Yang et al., 2021). Fig. 3 shows the FT-IR infrared spectra of Nd in the range of 4000–500 cm^{-1}, where 3418.6 cm^{-1} and 2969.8 cm^{-1} are broad absorption peaks with moderate intensity. The ─OH stretching vibration of tannin molecules contained in phenolic aldehyde and aliphatic structure is at 3418.6 cm^{-1}, and the small peak at 2969.8 cm^{-1} originated from the ─CH stretching vibration in aromatic methoxy and the side chain of methyl and methylene (Chupin et al., 2013). The carbonyl absorption peak is in the region of 1900–1600 cm^{-1}. Due to the stretching vibration of C═O and the influence of hydrogen bond, the C═O absorption in carboxyl group moves to a low wave. The peaks at 1621.8 cm^{-1} and 1384.6 cm^{-1} are attributed to C═C stretching vibration of α-linolenic acid, ─C─OH stretching vibration of phenolic acid, C═O stretching vibration of carboxyl group and ─CH deformation in flavonoid aromatic ring system. The peak at 1318.5 cm^{-1} was attributed to the out-of-plane bending vibration of C-H of olefin compounds. The peak at 1075.1 cm^{-1} and 619.5 cm^{-1} corresponded to the stretching vibration of ─CO and the plane bending vibration of the C─O bond of tannins (Ricci et al., 2015).
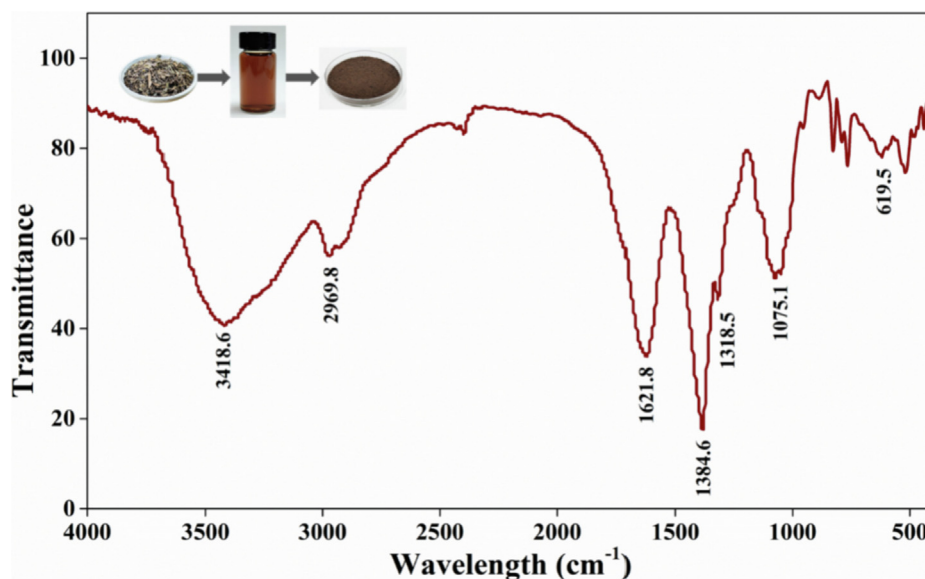

Fig. 3 FT-IR spectra of Nd powder.

3.2. Extract processes of Nd colorant

The parameters such as temperature, time, and bath ratio of wool fabric were optimized by a single factor experiment and the results are shown in Fig. 4. As shown, the absorbance increased with increasing temperature, and reached the maximum value at extraction temperature of 90 °C, however, it decreased with further increasing temperature. This is because the α-linolenic acid molecules primarily comprising ω-3 in Portulaca oleracea L. are easy to decompose under high temperature, which potentially disrupts the conjugated system of Nd and absorbance, thereby producing a deepening effect. Nonetheless, if the temperature was too high, it would destroy the structure of Portulaca oleracea L. and reduce absorbance (Ye et al., 2021). Therefore, the extraction temperature can be defined as 90 °C.

The absorbance increased with the extension of extract time within 1 h, whereas decreased with a further prolonged time. When the time is within 1 h and the time is short, the extraction of Portulaca oleracea L. is not sufficient. If the time exceeds 1 h, it may cause the decomposition of colorant, which is not conducive to the extraction. The time should be controlled within a certain range. Under this condition, it is more appropriate to select the extraction time of about 1 h. The absorbance of Nd at a bath ratio of 1:20–1:30 was higher than that of a large bath ratio due to the higher Nd and more tannins obtained per unit mass of deionized water at a low bath ratio.

Through single factor experiment, SPSS was designed for the factors that have a great impact on Portulaca oleracea L.

pigment, namely extraction temperature, extraction time and solid–liquid ratio. The test scheme is shown in Table 1.

Through single factor experiment, the better three levels under each factor were selected for three factor and three level SPSS design to screen the best extraction conditions of Portulaca oleracea L. The extraction effect is analyzed according to the value of each factor, as shown in Table 2. The results show that the best extraction conditions are: temperature 100 °C, time 1.5 h and bath ratio 1:20.

Fig. 4(d) is mainly used to test the acid resistance stability of the extracted oleracea L. solution. The initial pH value of nature dye solution was recorded as 7. First of all, the absorption wavelength of the solution does not change with the change of pH, but always maintains the same position. Second, at the λ_{max} of 340 nm, the absorbance corresponding to each pH fluctuates regularly, and the absorbance value fluctuates around 1. It indicate that the acid resistance stability of the solution is very good and shows that acidic medium will not change the chemical composition and chromogenic group of Portulaca oleracea L., but promote the increase of release by improving the permeability of solvent and damage to plant tissue (Shelembe et al., 2014).

3.3. Dyeing conditions and exhaustion rate

As shown in Fig. 5(a) and Table 3, the color intensity of wool fabric decreasedwith increased pH value when the pH of the dyeing bath was below the isoelectric point of wool of 4.2–4.8 due to the existing coulomb force and Van der Waals force.
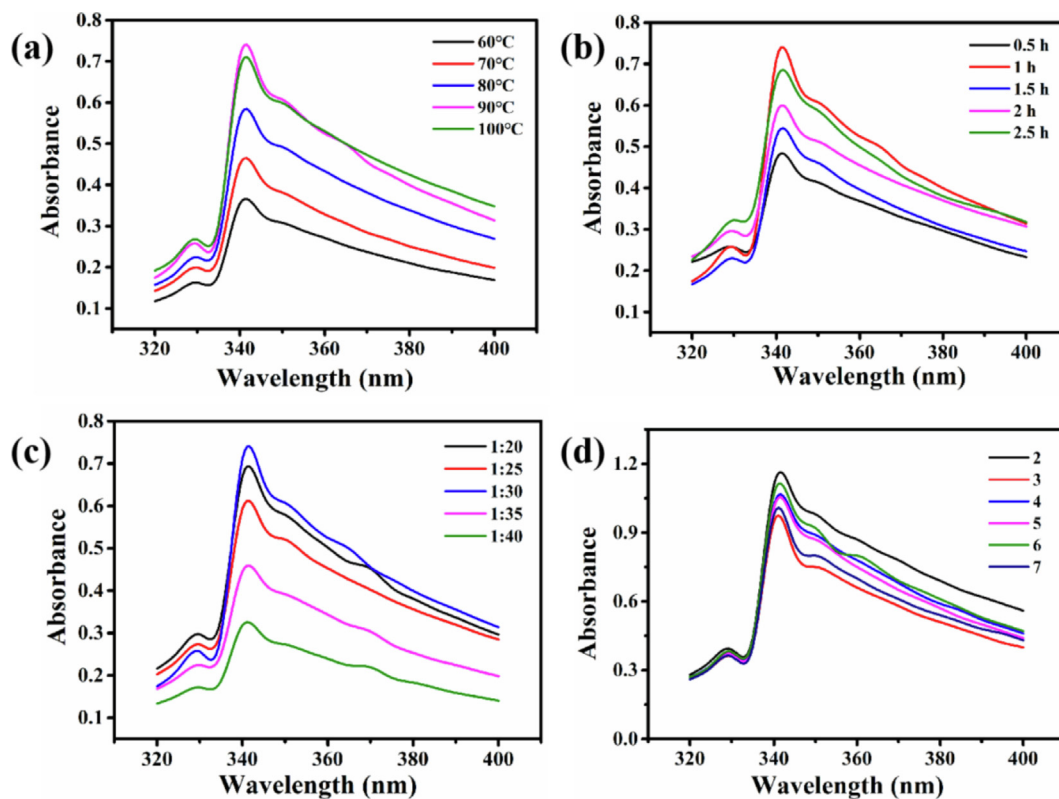
Fig. 4 UV–vis spectral analysis for the absorbance of Nd extracted by the conditions: (a) different temperatures under 1 h and 1:30; (b) different times under 1 h and 90 °C; (c) different bath ratios under 1 h and 90 °C. (d) Stability of extracted Nd solution under acidic conditions.

In contrast, the dye uptake decreased with a further increased pH value when the pH was higher than 4.8 (Zhou et al., 2020). As shown in Fig. 5(b), the maximum exhaustion rate was 35.67% at 90 °C. The increase in temperature promotes the swelling of the wool fiber; this is conducive to the further diffusion of Nd into the wool fiber. When the temperature exceeds 60 °C, the disulfide bond in the macromolecular structure of wool begins to open, and the reaction activity between the colorant and wool fabric is simultaneously enhanced. A reasonable increase in dyeing time would help in the increase of Nd exhaustion rate (Fig. 5(c)); the dyeing rate cannot significantly increase when the dyeing time is higher than 75 min. Fig. 5(d) shows that the increase of bath ratio would increase the number of Nd molecules in dye solution, which will improve the binding rate with wool fabric. When the liquor ratio is 1:35, the dye exhaustion rate reaches the maximum. Nevertheless, the adsorbed capacity of remaining Nd in dye solution would decrease after adequate adsorption on the surface of wool fabric. Therefore, if continue to increase the bath ratio and dye content, the adsorption capacity of the wool fabric will decrease instead.

Through single factor experiment, the factors that have great influence on dyeing were designed, namely dyeing pH, temperature, time and solid–liquid ratio. The test scheme is shown in Table 4.

Table 2 Extraction effects of different extraction factors on pigment.

	Tem. (°C)	Time (h)	Ratio	Absorbance
1	1	1	1	0.76
2	1	2	2	0.57
3	1	3	3	0.43
4	2	1	2	0.51
5	2	2	3	0.43
6	2	3	1	0.52
7	3	1	3	0.79
8	3	2	1	1.26
9	3	3	2	0.79
K_1	1.76	2.06	2.54	
K_2	1.45	2.25	1.86	
K_3	2.84	1.74	1.64	
k_1	0.58	0.69	0.85	
k_2	0.48	0.75	0.62	
k_3	0.95	0.58	0.55	
R	0.46	0.17	0.30	

Note: K is the sum of the test results of each factor level. For example, K1 is the sum of the absorbance corresponding to level 1, that is, K1 = 0.76 + 0.57 + 0.43 = 1.76; k is the mean value of the sum of factor test results; R is the range of K value under each factor.

The dyeing effect was analyzed based on the value of each factor, and SPSS design was applied (Table 5). The findings show the optimum dyeing process of pH = 2, temperature 100 °C, time 1.5 h, solid–liquid bath ratio 1:35, and the dye uptake of up to 43.79%.

3.4. Adsorption dynamics

Based on the single factor experimental results of natural dye dyeing, a suitable adsorption system was selected, and the temperatures were regulated at 80 °C, 90 °C, and 100 °C. Fig. 6(a) reveals that the adsorption capacity of the wool fabric significantly increases within the first 40 min. After dyeing for 40 min, the adsorption rate decreased from 1.3205 kg/g/min to 7.828×10^{-2} kg/g/min, and the equilibrium time was about 120 min. To comprehensively understand the adsorption kinetics, the adsorption kinetics equation, pseudo-first-order, and pseudo-second-order models were utilized to further analyze the adsorption features and influencing factors (Shen et al., 2014).

For pseudo-first-order dynamics, the linearized rate equation was calculated using the Formula (5):

$$\ln q_e - q_t = \ln q_e - K_1 t \tag{5}$$

where q_e (g/kg wool) and q_t (g/kg wool) represent the rate constants of dyes adsorbed on wool fibers at equilibrium and time t, respectively. The pseudo-second-order rate equation is as follows (Barros et al., 2013):

$$\frac{t}{q_t} = \frac{1}{K_2 q_e^2} + \frac{1}{q_e} t \tag{6}$$

In the equation, K_2 (kg/g/min) is the equilibrium rate constant of the pseudo-second-order process. The linear changes of ln $(q_e\text{-}q_t)$ and tq_t verses t (min) was analyzed by nonlinear least square regression, which confirms the applicability and fitting of the above two dynamic models. The rate constant (k_2) and equilibrium adsorption capacity (q_e) were calculated using the slope and intercept of the linearized Equation (Kayodé et al., 2012). In addition, the adsorption rate and half-staining time $(t_{1/2})$ are calculated using Formulas (7) and (8):

$$r_i = k_2 q_e^2 \tag{7}$$

$$t_{1/2} = \frac{1}{k_2 q_e} \tag{8}$$

Generally, the pseudo-first-order kinetic model is suitable for describing the initial stage of adsorption, while the pseudo-second-order kinetic model describes the whole adsorption process. Table 5 demonstrates that the R^2 of the pseudo-second-order kinetic model is above 0.997, indicating that the adsorption process of Nd on WF is increasingly in line with the pseudo-second-order kinetic adsorption model. Besides, it illustrates that the adsorption process is primarily regulated by chemical adsorption accompanied by electrostatic force, hydrogen bond, and ion–dipole interaction (Zhang et al., 2017). As shown in Table 6, when the temperature is further increased from 90 °C to 100 °C, the adsorption capacity increases from 25.991 g/kg to 44.067 g/kg, suggesting that the equilibrium is immediately attained at 100 °C compared
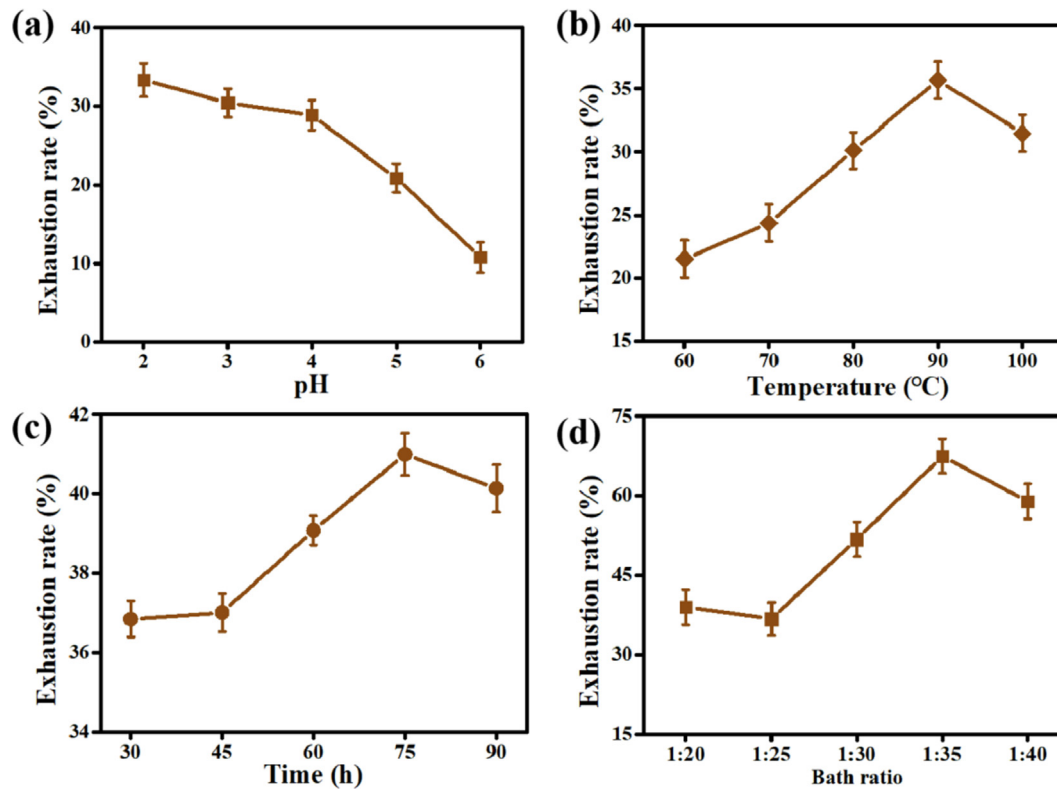
Fig. 5 The effect of conditions on dye exhaustion rate:(a) pH values with other conditions: 90 °C, 1 h and 1:20; (b) Temperatures with other conditions: pH 2, 1 h and 1:20; (c) Times with other conditions: pH 2, 90 °C and 1:20; (d) Bath ratio with other conditions: pH 2, 90 °C, 75 min.

Table 3 Effect of dyeing process factors on color intensity.

pH	K/S	Tem.(°C)	K/S	T(min)	K/S	Ratio	K/S
pH = 2	15.85	60	12.352	30	17.464	1:20	13.68
pH = 3	14.122	70	16.022	45	17.881	1:25	13.102
pH = 4	13.898	80	16.808	60	17.601	1:30	16.376
pH = 5	12.984	90	21.635	75	20.379	1:35	17.262
pH = 6	11.873	100	16.376	90	18.318	1:40	16.256

Table 4 Factors and levels of dyeing conditions.

	pH. A	Tem. B (°C)	T. C (h)	Ratio. D
1	2	80 °C	60 min	1:30
2	3	90 °C	75 min	1:35
3	4	100 °C	90 min	1:40

to 80 °C and 90 °C. The initial adsorption rate r_i (g/kg/min) increases with increasing temperature, resulting in the decrease of $t_{1/2}$ (min).

As shown in Table 7, the sequence of color intensity (K/S value) of different dyeing methods is MF > NF > SF > WF. According to the literature, the use of mordant improves the combination of dye and fiber; the fiber can attain a stable color (Vankar et al., 2008). The

higher K/S value and darker color of the sample are attained after dyeing with natural mordant as shown in Fig. 6(c).

3.5. Chemical analysis of fabrics

The FT-IR spectrums of WF, NF, and MF were significantly similar (Fig. 7(a)), indicating that the overall structure of wool fabric dyed with Nd and Md remained undamaged. Notably,

Table 5 Orthogonal experiment SPSS design.

	pH	Tem. (°C)	Time(h)	Ratio	Exhaustion rate (%)
1	1	1	1	1	28.42
2	1	2	2	3	28.56
3	1	3	3	2	43.79
4	2	1	2	2	4.19
5	2	2	3	1	14.44
6	2	3	1	3	22.82
7	3	1	3	3	7.27
8	3	2	1	2	9.86
9	3	3	2	1	6.38
K1	94.2	39.88	61.10	49.24	
K2	41.45	52.86	39.13	51.27	
K3	23.51	69.90	58.93	58.65	
k_1	31.40	13.293	20.367	16.413	
k_2	13.817	17.62	13.043	17.09	
k_3	7.837	23.30	19.643	19.55	
R	23.563	10.007	7.324	2.460	

Note: K is the sum of the test results of each factor level. For example; k is the mean value of the sum of factor test results; R is the range of K value under each factor.
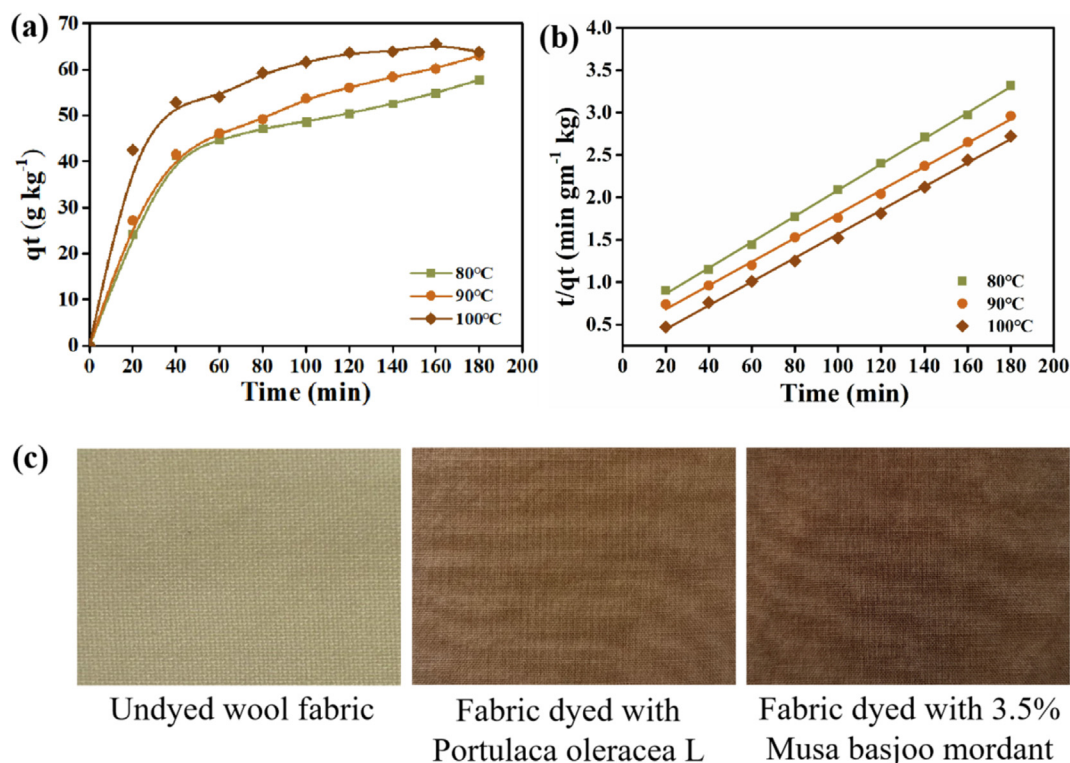
Fig. 6 (a) Kinetic curves of dyeing wool fabric with Nd at different temperatures; (b) pseudo-second-order fitting line; (c) Comparison of wool fabrics dyed with different methods.

near 3280 cm^{-1} in the infrared spectrum is the coupling of -NH stretching vibration and amide stretching vibration, which is related to the change of force caused by hydrogen bond breaking between molecular chains. When the hydrogen bond between molecular chains breaks, the electron cloud density of C in C—H decreases, causing a shift in the stretching vibration band of C—H. To highlight the small differences that are difficult to detect, NF and MF infrared spectra were subtracted from WF infrared spectra, respectively (Fig. 7(b)) to eliminate the interference of background spectra and similar conditions. In the difference spectrum, COO$^-$ and —OH in natural dyes are combined with —NH$_2$ or —CO—NH on protein fibers to enhance the hydrogen bond between natural dyes and wool. Among them, 1631 cm^{-1} and 1647 cm^{-1} are carboxyl stretching vibration regions, and 3750–3000 cm^{-1} are O—H and N—H stretching vibration regions. Therefore, the correspond-

Table 6 Kinetic parameters of Nd adsorption on wool fabric.

Pseudo-first-order model				Pseudo-second-order model				
Tem (°C)	q_{e1} (g/Kg)	R^2	k_1 (kg/g/min)	q_{e2} (g/Kg)	R^2	k_2 (kg/g/min)	r_i (g/kg/min)	$t_{1/2}$ (min)
80	15.141	0.9653	3.208×10^{-1}	10.746	0.9991	1.526×10^{-2}	1.762	6.098
90	25.991	0.9732	3.501×10^{-1}	13.345	0.9975	1.4×10^{-2}	2.493	5.352
100	44.067	0.9040	3.543×10^{-1}	20.791	0.9979	1.402×10^{-2}	6.060	3.431

Table 7 Color Eigenvalues and Strength of Dyed Fabrics.

| Item	Colorfastness to				K/S	L^*	a^*	b^*	C^*	h^o
	Wash	Dry rubbing	Wet rubbing	Light						
WF				3–4	12.9	82.4	1.75	2.67	3.19	56.7
NF	4	4	3–4	3–4	21.1	49	9.63	23.05	24.98	67.33
MF	4	4–5	3–4	4	23.5	43	8.75	20.74	22.51	67.12
SF	4–5	4–5	4–5	4–5	21.1	49.24	9.82	22.97	25.11	67.37
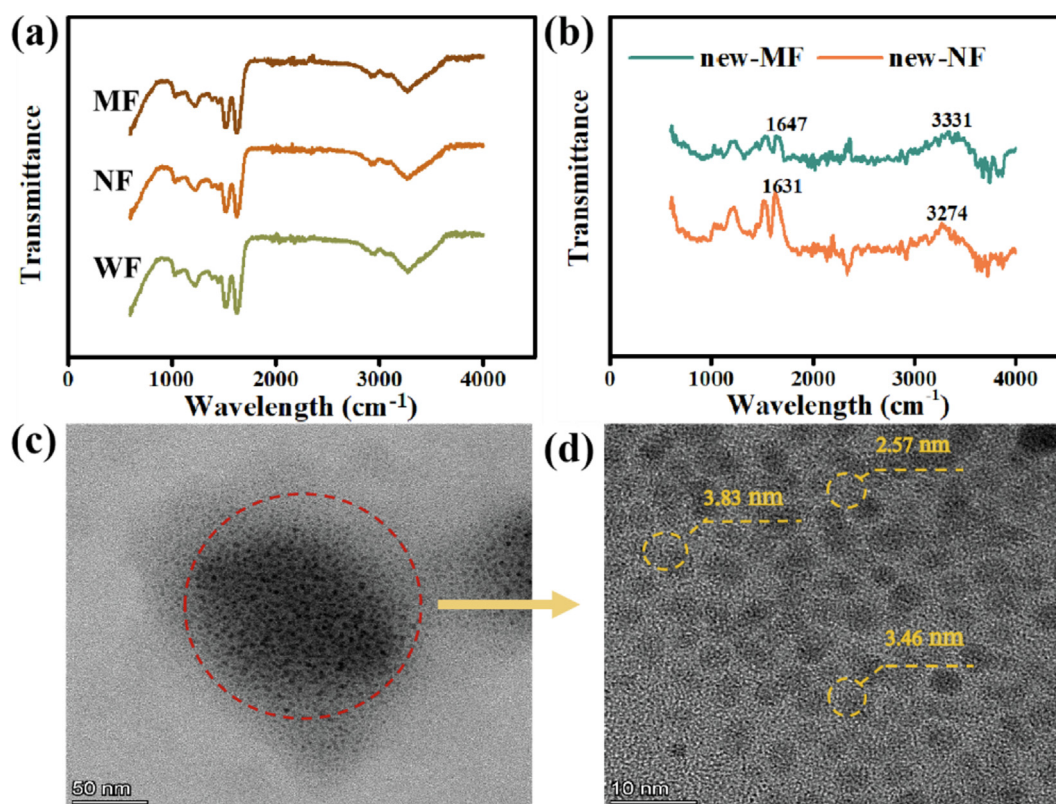
Fig. 7 (a) Infrared spectrum of three dyed fabric samples; (b) Infrared difference spectrum of MF and NF; (c) and (d): TEM images of Nd solution.

ing characteristics of the absorption peak are gradually enhanced (Yrab et al., 2019).

The dye colorants exist in black spot-like aggregates with a diameter of 100 nm–150 nm (Fig. 7b). Unlike other natural dyes with the particle size of 2–4 μm (Lbkma et al., 2021; Li et al., 2021; Zhang et al., 2019), the dye aggregates comprise dozens to hundreds of nanoscale particles and the particle size

of about 2.98 ± 0.54 nm (Fig. 7(c)); this is similar to the size of quantum dots. Thus, the colorant particles could be effectively and evenly dispersed in water and diffused into the wool fabric to attain a high exhaustion rate and color intensity (K/S).

The SEM images in Fig. 8(a-c) show the surface morphology of different wool fabrics without an apparent difference, suggesting that the dyeing process would not alter the surface
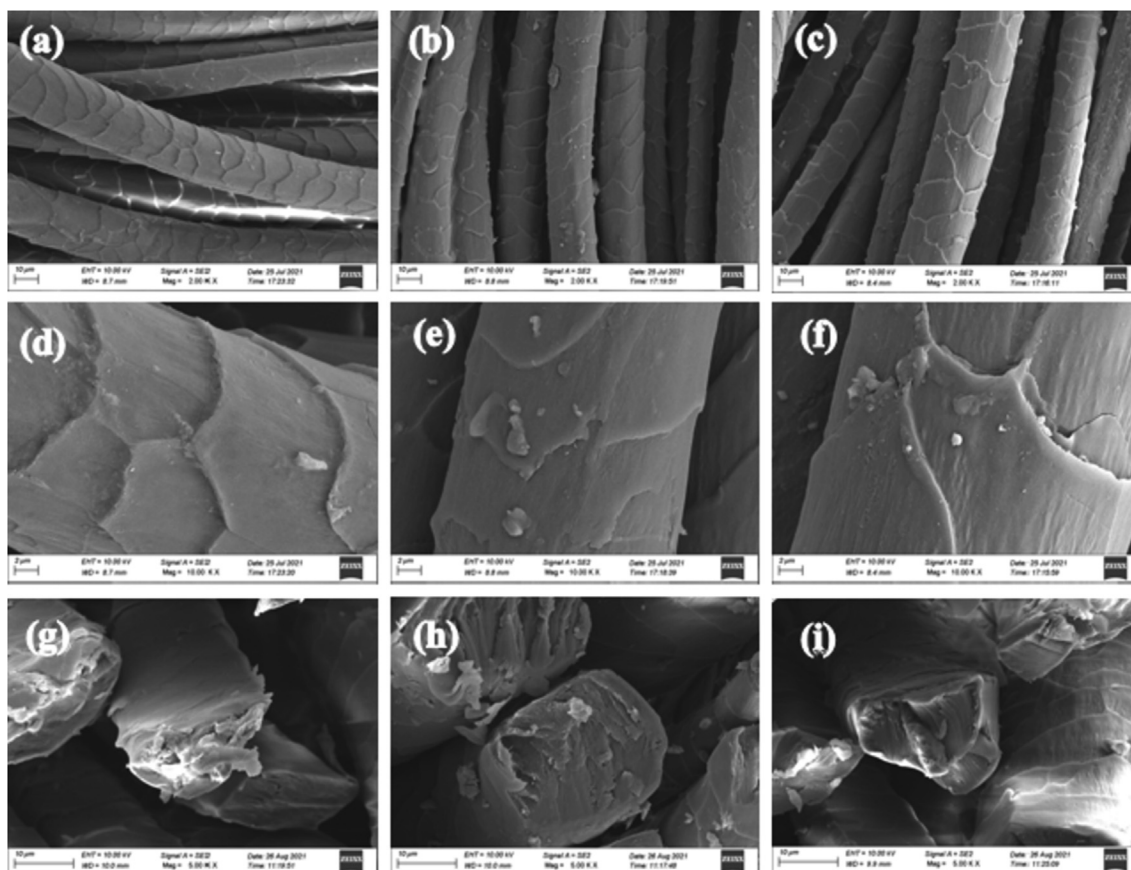
Fig. 8 SEM images of fabric samples :(a) WF × 2 K; (b) NF × 2 K; (c) MF × 2 K; (d) WF × 10 K; (e) NF × 10 K; (f) MF × 10 K; (g), (h) and (i): Cross section electron microscope of wool WF, NF and MF.
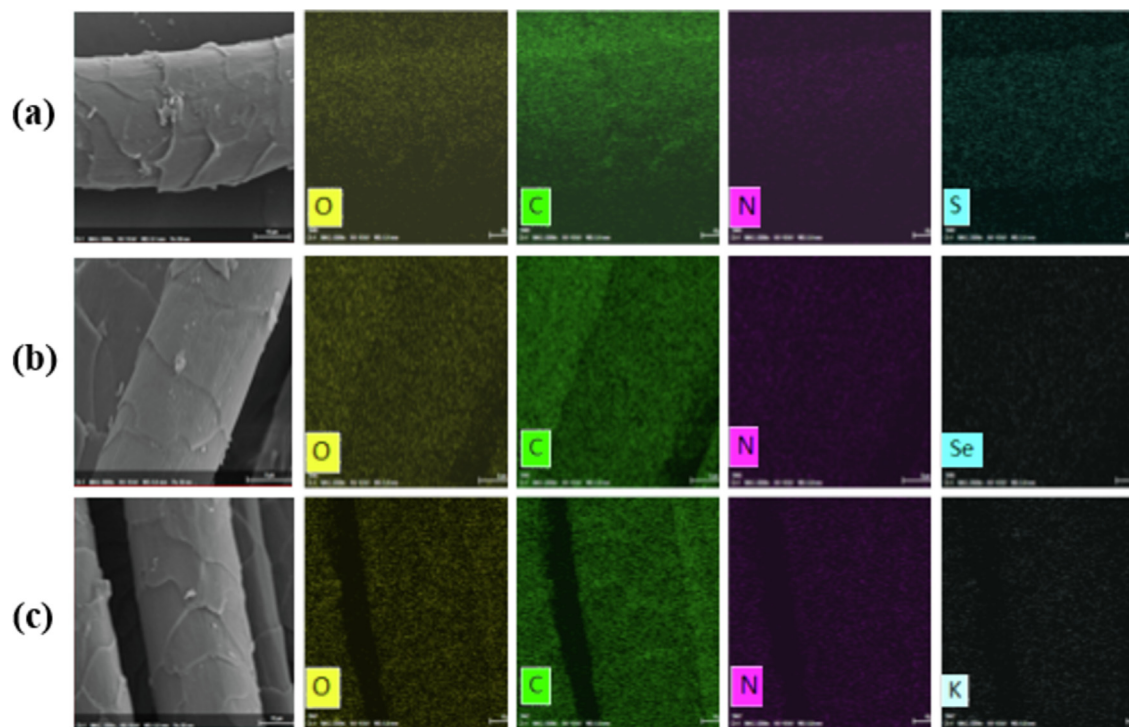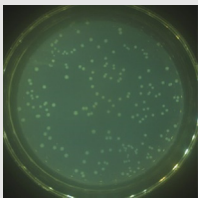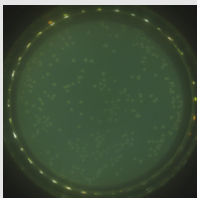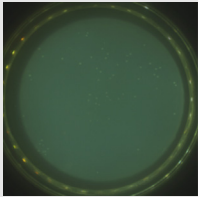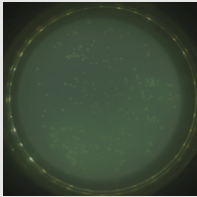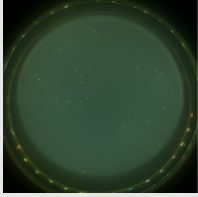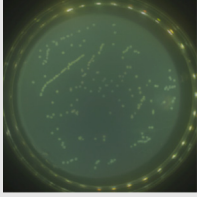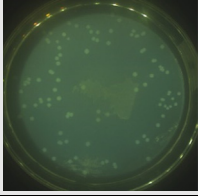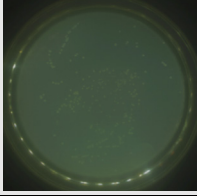

Fig. 9 EDS analysis of fabrics: (a) WF; (b) NF; (c) MF.

Table 8 UV protection performance of dyeing and standard samples.

	Transmittance		UPF values	Antioxidant	Error
	T (UVA)	T (UVB)			
WF	0.84	0.62	153.29	19.2%	4.2%
NF	0.47	0.43	229.05	25.3%	4.8%
MF	0.42	0.39	253.47	32.0%	5.1%
SF	0.41	0.40	248.92	24.8%	6.4%

Table 9 Antibacterial activity of fabrics against *S. aureus* and *E. coli*.

S. No.	*S. aureus*	*E. coli*	Antibacterial rates against *S. aureus* / *E. coli*	Error
WF			–/–	–/–
NF			47.8%/12.5%	6.8%/4.5%
MF			71.3%/37.0%	5.6%/3.9%
SF			25.2%/11.8%	7.2%/4%

morphology of the fabrics. The smooth fiber with a clear scale layer structure is shown on the surface of WF (Fig. 8(d)). However, the images in Fig. 8(e) and (f) show that the scale layer of wool fiber is destroyed, which would promote the diffusion of dye molecules into the fiber and significantly improve the efficiency of dyeing. Fig. 8(g-i) shows the cross-sectional of WF, NF, and MF. Of note, the material is solid and will not lose its capillary structure in the fiber due to expansion. These capillary structures ensure satisfactory diffusion characteristics.

Fig. 9 shows the distribution of elements in undyed and dyed WFs. Because of the presence of Se in Portulaca oleracea L., K in Musa basjoo leaves, Se and K appearing in Fig. 9(b) and (c) further verifies that natural dyes and mordants have been successfully dyed on WFs. The carbon–oxygen ratios

(C/O) of WF, NF, and MF are 2.49, 2.67, and 2.85, respectively. MF samples have higher C/O and higher color intensity. The weight percentage of carbon and oxygen confirms the presence of hydroxylated flavonoids and catechin derivatives, which in turn verifies that the natural mordants rich in tannins cause the adsorption of fibers and dyes, and the excellent C/O improves the bioactivity of dyed fabrics (Hosseinzadeh et al., 2021; Rather et al., 2021).

3.6. UV protection and antioxidant properties

Due to the presence of quercetin, the number of functional groups including phenolic groups on the surface of fabric increased after Nd dyeing, thereby enabling NF and MF samples to have a better antioxidant capacity (Lu et al., 2018; Diao

et al., 2021). The transmittance of UVA and UVB radiation depends on the type and degree of chemical interaction between wool fabric and natural dyes. As shown in Table 8, the UPF of WF is 153.29; this is classified as excellent. The dyed fabrics demonstrated lower transmittance (blocking ultraviolet radiation) and higher UPF values than that of the control samples, hence determining the superior UV resistance (Shabbir et al., 2018).

3.7. Antibacterial properties

S. aureus and *E. coli* colonies in the dyed fabric were lower than that in the blank control group; *S. aureus* was significantly reduced on the MF in Table 9. This is because α-linolenic acid, quercetin, coumarin, catechin, and other components exhibit certain antibacterial abilities. Quercetin inhibits DNA and RNA synthesis in bacterial cells and interferes with cell membrane activity (Yl et al., 2021). Coumarinic acid exhibits effective antibacterial activity against *E. coli* and *S. aureus*; it inhibits cell proliferation resulting in apoptosis (Lu et al., 2018; Ren et al., 2021). The phenolic hydroxyl groups in the catechins molecule are combined with peptide bonds, amino and carboxyl groups in bacterial cell membrane proteins, resulting in membrane protein denaturation and further bacterial death (Ben et al., 2015; Ren et al., 2016). The antibacterial rate of wool fabric increased after mordant dyeing, specifically for *S. aureus* (71.3%); this confirms that the chemical reaction of Nd has a significant effect on its antibacterial activity.

4. Conclusion

This study explored the high color yield and bioactive finishing of wool fabric with Portulaca oleracea L. as a natural dye, evaluated its dyeing properties and dyeing kinetics, and understood its dyeing mechanism. Natural dye molecules have good stability in acid and high temperature. Due to the nano particle size, they are evenly dispersed in the aqueous solution, which further improves the dyeing strength and fastness. In addition, the adsorption process of wool fabric on natural colorant molecules conforms to the quasi second-order kinetic adsorption model. In addition, the dyeing effect of wool fabric was compared with that of Musa basjoo mordant and synthetic dye. After the natural mordant added to the dye solution, the mordant and the dye migrate to the fiber surface and are adsorbed, and then dynamically diffuse to the fiber for bonding. The results showed that Portulaca oleracea L. dye and natural mordant worked together to make the fabric have superior color depth (K/S value 23.53) and biological functions, such as UV resistance (UPF value 253.47) and antibacterial activity (antibacterial rate of *S. aureus*/*E. coli* is 71.3%/37%). As a functional natural dye, Portulaca oleracea L. is a potential substitute in textile and garment industry.

Declaration of Competing Interest

The authors declare no known competing financial interests or personal relationships that could have appeared to affect the study.

Acknowledgment

References

Aludatt, M.H., Rababah, T., Alhamad, M.N., Tawaha, A., Al-Tawaha, A.M., 2020. Herbal yield, nutritive composition, phenolic contents and antioxidant activity of purslane (Portulaca oleracea L.) grown in different soilless media in a closed system. Ind. Crops Prod. 141, 111746.

Baliarsingh, S., Panda, A.K., Jena, J., Das, T., Das, N.B., 2012. Exploring sustainable technique on natural dye extraction from native plants for textile: identification of colourants, colourimetric analysis of dyed yarns and their antimicrobial evaluation. J. Cleaner Prod. 37, 257–264.

Barros, F., Dzkes, L., Awika, J.M., Roonez, L.W., 2013. Accelerated solvent extraction of phenolic compounds from sorghum brans. J. Cereal Sci. 58, 305–312.

Ben, S., Rihab, F., Khaled, B., Ticha, M., El, K., 2015. Mixture approach for optimizing the recovery of colored phenolics from red pepper (Capsicum annum L.) by-products as potential source of natural dye and assessment of its antimicrobial activity. Ind. Crops Prod. 70, 34–40.

Cano, A., Contreras, C., Chiralt, A., González-Martínez, C., 2021. Using tannins as active compounds to develop antioxidant and antimicrobial chitosan and cellulose based films. Carbohydr. Polym. Technol. Appl. 2, 100156.

Chupin, L., Motillon, C., Bouhtoury, C.E., Pizzi, A., Charrier, B., 2013. Characterisation of maritime pine (Pinus pinaster) bark tannins extracted under different conditions by spectroscopic methods, FTIR and HPLC. Ind Crops Prod. 49, 897–903.

Desta, M., Molla, A., Yusuf, Z., 2020. Characterization of physico-chemical properties and antioxidant activity of oil from seed, leaf and stem of purslane (Portulaca oleracea L.). Biotechnol. Rep. 27, e00512.

Diao, M., Liang, Y., Zhao, J., Zhao, C., Zhang, T., 2021. Enhanced cytotoxicity and antioxidant capacity of kaempferol complexed with α-lactalbumin. Food Chem. Toxicol. 153, 112265.

Eid, B.M., Ibrahim, N.A., 2020. Recent developments in sustainable finishing of cellulosic textiles employing biotechnology. J. Cleaner Prod. 284, 12470.

Hosseinzadeh, M.H., Ghalavand, A., Boojar, M.A., Modarres-Sanavy, S., Mokhtassi-Bidgoli, A., 2021. Application of manure and biofertilizer to improve soil properties and increase grain yield, essential oil and ω3 of purslane (Portulaca oleracea L.) under drought stress. Soil Tillage Res. 205, 104633.

Iba, B., Cg, C., Ap, C., Om, B., Laa, D., Amm, A., Rea, D., 2020. Phytochemical screening and DPPH radical scavenging activity of three morphotypes of Mauritia flexuosa L.f. from Peru, and thermal stability of a milk-based beverage enriched with carotenoids from these fruits. Heliyon. 6, e05209.

Ibrahim, N.A., El-Zairy, M.R., Eid, B.M., El-Zairy, E., Emam, E.M., 2015. New finishing possibilities for producing durable multifunctional cotton/wool and viscose/wool blended fabrics. Carbohydr. Polym. 119, 182–193.

Kang, G., Yi, P., Ljra, B., Wwa, B., Qi, Z., Tza, B., Qla, B., 2019. Natural pigment during flora leaf senescence and its application in dyeing and UV protection finish of silk and wool – a case study of Cinnamomum Camphora. Dyes Pigm. 166, 114–121.

Kayodé, A.P.P., Bara, C., Dalodé-Vieira, G., Linnemann, A.R., Nout, M., 2012. Extraction of antioxidant pigments from dye sorghum leaf sheaths. LWT-Food Sci. Technol. 46, 49–55.

Kenawy, E.R., Worley, S., Broughton, R., 2007. The chemistry and applications of antimicrobial polymers: a state-of-the-art review. Biomacromolecules 8, 1359–1384.

Mancilio, L.B.K., Ribeiro, G.A., de Almeida, E.J.R., de Siqueira, G.M.V., Rocha, R.S., Guazzaroni, M.E., De Andrade, A.R., Reginatto, V., 2021. Adding value to lignocellulosic byproducts by using acetate and p-coumaric acid as substrate in a microbial fuel cell. Ind. Crops Prod. 171, 113844.

Li, S., Zhou, S., Zhao, G., 2021. Tuning the morphology of micro- and nano-spheres from bamboo shoot shell acetosolv lignin. Ind. Crops Prod. 171, 113860.

Lm, A., Ht, A., Yu, P.A., Sw, A., Zz, A., Es, B., Sd, C., Gz, D., Wsc, A., Yw, A., 2019. The anti-inflammatory potential of Portulaca oleracea L. (purslane) extract by partial suppression on NF-κB and MAPK activation. Food Chem. 290, 239–245.

Lu, C., Li, C., Chen, B., Shen, Y., 2018. Composition and antioxidant, antibacterial, and anti-HepG2 cell activities of polyphenols from seed coat of Amygdalus pedunculata Pall. Food Chem. 265, 111–119.

Luo, X., White, J., Thompson, R., Rayner, C., Kulik, B., Kazlauci-unas, A., He, W., Lin, L., 2018. Novel sustainable synthesis of dyes for clean dyeing of wool and cotton fibres in supercritical carbon dioxide. J. Cleaner Prod. 199, 1–10.

Mathur, J.P., Gupta, N.P., 2003. Use of natural mordant in dyeing of wool. Indian J. Fibre Text. Res. 28, 90–93.

Mr, A., Mm, B., Abr, B., Mmr, C., 2021. Facile technique for wool coloration via locally forming of nano selenium photocatalyst imparting antibacterial and UV protection properties. J. Ind. Eng. Chem. 101, 153–164.

Nemzer, B., Al-Taher, F., Abshiru, N., 2020. Phytochemical compo-sition and nutritional value of different plant parts in two cultivated and wild purslane (Portulaca oleracea L.) genotypes. Food Chem. 320, 126621.

Oh, W.Y., Ambigaipalan, P., Shahidi, F., 2021. Quercetin and its ester derivatives inhibit oxidation of food, LDL and DNA. Food Chem. 364, 130394.

Pereira, A., Maraschin, M., 2015. Banana (Musa spp) from peel to pulp: ethnopharmacology, source of bioactive compounds and its relevance for human health. J. Ethnopharmacol. 160, 149–163.

Petropoulos, S., Karkanis, A., Martins, N., Ferreira, I., 2016. Phytochemical composition and bioactive compounds of common purslane (Portulaca oleracea L.) as affected by crop management practices. Trends Food Sci. Technol. 55, 1–10.

Rather, L.J., Akhter, S., Padder, R.A., Hassan, Q.P., Hussain, M., Khan, M.A., Mohammad, F., 2017. Colorful and semi durable antioxidant finish of woolen yarn with tannin rich extract of Acacia nilotica natural dye. Dyes Pigm. 139, 812–819.

Rather, L.J., Zhou, Q., Ali, A., Mohd, Q., 2021. Valorization of agro-industrial waste from peanuts for sustainable natural dye produc-tion: focus on adsorption mechanisms, ultraviolet protection, and antimicrobial properties of dyed wool fabric. ACS Food Sci. Technol. 1, 427–442.

Ren, Y., Fu, R., Fang, K., Xie, R., Shi, Z., 2021. Clean dyeing of acrylic fabric by sustainable red bacterial pigment based on nano-suspension system. J. Cleaner Prod. 281, 125295.

Ren, Y., Gong, J., Wang, F., Li, Z., Zhang, J., Fu, R., Lou, J., 2016. Effect of dye bath ph on dyeing and functional properties of wool fabric dyed with tea extract. Dyes Pigm. 134, 334–341.

Ricci, A., Olejar, K.J., Parpinello, G.P., Kilmartin, P.A., Versari, A., 2015. Application of Fourier Transform Infrared (FTIR) spec-troscopy in the characterization of tannins. Appl. Spectrosc. Rev. 50, 407–442.

Safapour, S., Sadeghi-Kiakhani, M., Eshaghloo-Galugahi, S., 2018. Extraction, dyeing, and antibacterial properties of crataegus elbursensis fruit natural dye on wool yarn. Fibers Polym. 19, 1428–1434.

Schaumlffel, L.S., Fontoura, L., Santos, S.J., Pontes, L.F., Gutterres, M., 2021. Vegetable tannins-based additive as antioxidant for biodiesel. Fuel 292, 120198.

Seif, M.M., Madboli, A.-N., Marrez, D.A., Aboulthana, W.M.K., 2019. Hepato-renal protective effects of egyptian purslane extract against experimental cadmium toxicity in rats with special emphasis

on the functional and histopathological changes. Toxicol. Rep. 6, 625–631.

Shabbir, M., Rather, L.J., Mohammad, F., 2018. Economically viable UV-protective and antioxidant finishing of wool fabric dyed with Tagetes erecta flower extract: valorization of marigold. Ind. Crops Prod. 119, 277–282.

Shahid, M., Shahid-ul-Islam, Mohammad, F., 2013. Recent advance-ments in natural dye applications: a review. J. Cleaner Prod. 53, 310–331.

Shelembe, J.S., Cromarty, D., Bester, M., Minnaar, A., Duodu, K.G., 2014. Effect of acidic condition on phenolic composition and antioxidant potential of aqueous extracts from sorghum (sorghum bicolor) bran. J. Food Biochem. 38, 110–118.

Shen, J., Gao, P., Ma, H., 2014. The effect of tris(2-carboxyethyl) phosphine on the dyeing of wool fabrics with natural dyes. Dyes Pigm. 108, 70–75.

Tang, Ren-Cheng, Zhou, Yuyang, Yang, Zhi-Yi, 2016. Bioactive and UV protective silk materials containing baicalin - The multifunc-tional plant extract from Scutellaria baicalensis. Georgi. Mater. Sci. Eng. C. 67, 336–344.

Vankar, P.S., Shanker, R., Mahanta, D., Tiwari, S.C., 2008. Ecofriendly sonicator dyeing of cotton with Rubia cordifolia Linn. using biomordant. Dyes Pigm. 76, 207–212.

Wang, Z., He, Z., Zhang, D., Li, H., 2020. Antioxidant activity of purslane extract and its inhibitory effect on the lipid and protein oxidation of rabbit meat patties during chilled storage. J. Sci. Food Agric. 2, 100156.

Yang, D.A., Zyb, C., Fan, H.A., Xy, A., Lj, C., Gyb, C., 2021. A new skeleton flavonoid and a new lignan from Portulaca oleracea L. and their activities. Fitoterapia 153, 104993.

Ye, D., Shen, L., Sun, Y., Zhang, D., Tan, X., Jing, P., Zhang, M., Tian, Q., 2021. Formulation and evaluation of a α-linolenic acid and vitamin E succinate microemulsion with low surfactant content and free of co-surfactant for use as a nutritional supplement. Food Chem. 364, 130433.

Yl, A., Lu, Z., Yxa, B., Zhi, C.C., Sy, A., By, A., Gl, A., Hg, B., Sl, A., Jwa, C., 2021. Antiviral activity of portulaca oleracea L. extracts against porcine epidemic diarrhea virus by partial suppression on myd88/NF-κb activation in vitro. Microb. Pathog. 154, 104832.

Ylj, A., Ly, A., Xfy, A., Rui, H.A., Sld, A., Xin, Y.A., Xu, L., Ylfa, B., 2021. The condensed tannin chemistry and astringency properties of fifteen Vitis davidii Foex grapes and wines. Food Chem.: X. 11, 100125.

Yrab, C., Rfab, C., Kfab, C., Wcab, C., Lhab, C., Rxab, C., Zhen, S., 2019. Dyeing cotton with tea extract based on in-situ polymeriza-tion: an innovative mechanism of coloring cellulose fibers by industrial crop pigments - ScienceDirect. Ind. Crops Prod. 142, 111863.

Zhang, W., Yao, J., Huang, P., Xing, S., 2019. Aqueous extraction of buckwheat hull and its functional application in eco-friendly dyeing for wool fabric. Text. Res. Journal 90, 1–14.

Zhang, X., Wang, Z., Wang, J., 2017. Adsorption kinetics of Cu^{2+} on nano alumina supported on activated carbon. Filtr. Sep. 27 (03).

Zhang, Y., Zhou, Q., Rather, L.J., Li, Q., 2021. Agricultural waste of Eriobotrya japonica L. (Loquat) seeds and flora leaves as source of natural dye and bio-mordant for coloration and bio-functional finishing of wool textile. Ind. Crops Prod. 169, 113633.

Zhou, Q., Rather, L.J., Ali, A., Wang, W., Li, Q., 2020. Environmental friendly bioactive finishing of wool textiles using the tannin-rich extracts of Chinese tallow (Sapium sebiferum L.) waste/fallen leaves. Dyes Pigm. 176, 108230.

Zhou, Y., Tang, R.C., 2017. Natural flavonoid-functionalized silk fiber presenting antibacterial, antioxidant, and UV protection perfor-mance. ACS Sustain. Chem. Eng. 5, 10518–10526.